Therapeutic targeting of LCK tyrosine kinase and mTOR signaling in T-cell Acute Lymphoblastic Leukemia

Tracking no: BLD-2021-015106R1

Saara Laukkanen (Tampere Center for Child, Adolescent and Maternal Health Research, Faculty of Medicine and Health Technology, Tampere University, Finland) Alexandra Bacquelaine Veloso (Massachussets General Hospital, United States) Chuan Yan (Massachusetts General Hospital, United States) Laura Oksa (Tampere Center for Child Health Research, Faculty of Medicine and Health Technology, Finland) Eric Alpert (Mass General Hospital Research Institute, United States) Daniel Do (Massachussets General Hospital, United States) Noora Hyvärinen (Tampere Center for Child Health Research, Faculty of Medicine and Health Technology, Finland) Karin McCarthy (Mass General Hospital Research Institute, United States) Abhinav Adhikari (Mass General Hospital Research Institute, United States) Qiqi Yang (Mass General Hospital Research Institute,) Sowmya Iyer (Mass General Hospital Research Institute, United States) Sara Garcia (Massachussets General Hospital, United States) Annukka Pello (Institute for Molecular Medicine Finland, Helsinki Institute of Life Science, Finland) Tanja Ruokoranta (Institute of Molecular Medicine Finland (FIMM), Finland) Sanni Moisio (The Institute of Biomedicine, School of Medicine, University of Eastern Finland, Finland) Sadiksha Adhikari (Institute for Molecular Medicine Finland, Helsinki Institute of Life Science, iCAN Digital Precision Cancer Medicine Flagship, Finland) Jeffrey Yoder (North Carolina State University, United States) Kayleigh Gallagher (University of Massachusetts Medical School, United States) Lauren Whelton (Mass General Hospital Research Institute, United States) James Allen (Mass General Hospital Research Institute, United States) Alexander Jin (Massachussets General Hospital, United States) Siebe Loontiens (Ghent University, Belgium) Merja Heinäniemi (University of Eastern Finland, Finland) Michelle Kelliher (University of Massachusetts Medical School, United States) Caroline Heckman (Tampere University Hospital, Tays Cancer Center, Finland) Olli Lohi (Tampere University Hospital, Tays Cancer Center, Finland) David Langenau (Mass General Hospital Research Institute, United States)

Abstract:
Relapse and refractory T cell acute lymphoblastic leukemia (T-ALL) has a poor prognosis and new combination therapies are sorely needed. Here, we used an *ex vivo* high-throughput screening platform to identify drug combinations that kill zebrafish T-ALL and then validated top drug combinations for preclinical efficacy in human disease. This work uncovered potent drug synergies between AKT/mTORC1 inhibitors and the general tyrosine kinase-inhibitor, dasatinib. Importantly, these same drug combinations effectively killed a subset of relapse and dexamethasone-resistant zebrafish T-ALL. Clinical trials are currently underway using the combination of mTORC1 inhibitor temsirolimus and dasatinib in other pediatric cancer indications, leading us to prioritize this therapy for preclinical testing. This combination effectively curbed T-ALL growth in human cell lines and primary human T-ALL and was well tolerated and effective in suppressing leukemia growth in patient-derived xenografts grown in mice. Mechanistically, dasatinib inhibited phosphorylation and activation of the lymphocyte-specific protein tyrosine kinase (LCK) to blunt the T-cell receptor (TCR) signaling pathway and when complexed with mTORC1 inhibition, induced potent T-ALL cell killing through reducing MCL-1 protein expression. In total, our work uncovered unexpected roles for the LCK kinase and its regulation of downstream TCR signaling in suppressing apoptosis and driving continued leukemia growth. Analysis of a wide array of primary human T-ALLs and PDXs grown in mice suggest that combination of temsirolimus and dasatinib treatment will be efficacious for a large fraction of human T-ALLs.

Conflict of interest: COI declared - see note

COI notes: C.A.H. has received research funding from Celgene, KronosBio, Novartis, Oncopeptides, Orion Pharma, and the IMI2 projects HARMONY and HARMONY PLUS unrelated to this study.

Preprint server: No;

Author contributions and disclosures: D.L., O.L., S.L. and A.V. conceived the study, S.L., A.V., C.Y., L.O., D.D, A.H.J., E.J.A., L.W., J.R.A., K.M., A.A. and N.H. conducted experiments, S. Lo. and J.Y. produced gateway plasmids, S.I, S.M, S.A and S.P.G. analyzed sequencing data, C.Y., K.G. and M.K. advised in animal experiments, A.P. assisted with primary patient samples, T.R. advised with the experimental design and data analysis of primary patient samples, C.A.H. provided primary patient samples and advised with the data, M.H. advised with data, D.L. and O.L. supervised the study. All authors reviewed and accepted the manuscript.

Non-author contributions and disclosures: No;

Agreement to Share Publication-Related Data and Data Sharing Statement: We provide patient sample data at the public deposit (osf.io/bk54u/)but also we are willing to provide other data by email (dlangenau@mgh.harvard.edu).

Clinical trial registration information (if any):

Therapeutic targeting of LCK tyrosine kinase and mTOR signaling in T-cell Acute Lymphoblastic Leukemia

Saara Laukkanen[1*], Alexandra Veloso [2,3,4,5*], Chuan Yan[2,3,4,5], Laura Oksa[1], Eric J. Alpert[2,3,4,5], Daniel Do[2,3,4,5], Noora Hyvärinen[1], Karin McCarthy[2,3,4,5], Abhinav Adhikari[2,3,4,5], Qiqi Yang[2,3,4,5], Sowmya Iyer[2,3,4,5], Sara P. Garcia[2,3,4,5], Annukka Pello[6], Tanja Ruokoranta[7], Sanni Moisio[8], Sadiksha Adhikari[6], Jeffrey A. Yoder[9], Kayleigh Gallagher[10], Lauren Whelton [2,3,4,5], James R. Allen[2,3,4,5], Alex H. Jin[2,3,4,5],Siebe Loontiens[11], Merja Heinäniemi[8], Michelle Kelliher[10], Caroline A. Heckman[6], Olli Lohi[1,13#], David M. Langenau[2,3,4,5#]

[1] Tampere Center for Child, Adolescent, and Maternal Health Research, Faculty of Medicine and Health Technology, Tampere University, 33520 Tampere, Finland; [2]Department of Pathology, , Charlestown, MA 02129, USA; [3]Center for Cancer Research, Massachusetts General Hospital, Charlestown, MA 02129, USA; [4]Harvard Stem Cell Institute, Boston, MA 02114, USA; [5]Center for Regenerative Medicine, Massachusetts General Hospital, Boston, MA 02114, USA; [6]Institute for Molecular Medicine Finland, Helsinki Institute of Life Science, iCAN Digital Precision Cancer Medicine Flagship, University of Helsinki, 00014 Helsinki, Finland; [7]Institute for Molecular Medicine Finland (FIMM), University of Helsinki, 00014 Helsinki, Finland, [8]The Institute of Biomedicine, School of Medicine, University of Eastern Finland, Kuopio, 70211, Finland; [9]Department of Molecular Biomedical Sciences, Comparative Medicine Institute, and Center for Human Health and the Environment, North Carolina State University, Raleigh, NC 27607, USA, [10]Department of Molecular, Cell and Cancer Biology, University of Massachusetts Medical School, Worcester, MA 01605, USA ;[11]Cancer Research Institute Ghent (CRIG) and Center for Medical Genetics, Ghent, Belgium; [13]Tampere University Hospital, Tays Cancer Center, 33520 Tampere, Finland

* Equal contribution
# Co-corresponding authors

Running title: Therapeutic targeting of tyrosine kinase signaling in T-ALL

Key points:

- Temsirolimus mTORC1 inhibitor and dasatinib kinase-inhibitor synergize to kill a large fraction of xenograft and primary human T-ALL
- The LCK kinase, which is inhibited by dasatinib, has unexpected roles in regulating TCR signaling pathways to drive continued T-ALL growth

Co-corresponding authors:

David M. Langenau, PhD
Dept. of Pathology, Harvard Medical School
Associate Chief of Research for Pathology,
Massachusetts General Hospital
149 13th Street, office #6012
Charlestown, Massachusetts 02129
dlangenau@mgh.harvard.edu
617-643-6508

Olli Lohi, MD, PhD
Tampere University, Faculty of Medicine
and Health Technology
Arvo Ylpön Katu 34,
33520, Tampere, Finland
olli.lohi@tuni.fi
+358 50 3186 249

ABSTRACT

Relapse and refractory T cell acute lymphoblastic leukemia (T-ALL) has a poor prognosis and new combination therapies are sorely needed. Here, we used an *ex vivo* high-throughput screening platform to identify drug combinations that kill zebrafish T-ALL and then validated top drug combinations for preclinical efficacy in human disease. This work uncovered potent drug synergies between AKT/mTORC1 inhibitors and the general tyrosine kinase-inhibitor, dasatinib. Importantly, these same drug combinations effectively killed a subset of relapse and dexamethasone-resistant zebrafish T-ALL. Clinical trials are currently underway using the combination of mTORC1 inhibitor temsirolimus and dasatinib in other pediatric cancer indications, leading us to prioritize this therapy for preclinical testing. This combination effectively curbed T-ALL growth in human cell lines and primary human T-ALL and was well tolerated and effective in suppressing leukemia growth in patient-derived xenografts grown in mice. Mechanistically, dasatinib inhibited phosphorylation and activation of the lymphocyte-specific protein tyrosine kinase (LCK) to blunt the T-cell receptor (TCR) signaling pathway and when complexed with mTORC1 inhibition, induced potent T-ALL cell killing through reducing MCL-1 protein expression. In total, our work uncovered unexpected roles for the LCK kinase and its regulation of downstream TCR signaling in suppressing apoptosis and driving continued leukemia growth. Analysis of a wide array of primary human T-ALLs and PDXs grown in mice suggest that combination of temsirolimus and dasatinib treatment will be efficacious for a large fraction of human T-ALLs.

INTRODUCTION

T-cell acute lymphoblastic leukemia (T-ALL) affects thousands of children and adults each year, and its incidence is increasing in the United States[1]. It is classified into at least seven distinct molecular subtypes based on their differences in transcription factor activation and arrest at different stages of T cell development[2–4]. Despite the wide array of oncogenic drivers that initiate this disease, leukemic cells also rely on activation of common pathways for leukemic cell transformation and progression. For example, the PI3K/AKT/mTORC1 pathway is active in a large fraction of T-ALL and elevates cell proliferation, increases stem cell number, and is strongly associated with treatment resistance[5–10]. This pathway is also acquired during evolution of T-ALL as a resistance mechanism to dexamethasone corticosteroid therapy[8,11–13]. Indeed, refractory and relapse disease, especially in the context of dexamethasone-resistance, are the major challenge facing patients. Only 30% of children and less than 10% of adults with refractory and relapse disease will survive[1,10]. Therefore, developing new treatments that efficiently kill refractory and relapse T-ALL is a top clinical imperative.

Lymphocyte-specific protein tyrosine kinase (LCK) is required for T cell development and maturation[14,15]. For example, LCK null mice fail to develop mature T cells and arrest at the CD4-, CD8- (CD44-, CD25+, DN3 stage) stage of thymocyte maturation. These arrested lymphocytes are unable to signal through the T-cell receptor (TCR) and subsequently die in the absence of positive selection[16]. Mature T lymphocytes also utilize LCK to regulate T cell receptor-mediated responses to antigen, ultimately regulating downstream phosphorylation programs that drive differentiation, proliferation and/or cytokine secretion[17,18] . Despite important roles for LCK in regulating normal T cell development and its necessity for downstream TCR phosphorylation signaling, its roles in T-ALL are not well understood. Indeed, T-ALLs are arrested during a wide array of T cell maturation stages, universally express activated LCK irrespective of subtype or mutational spectrum, and yet, many T-ALLs lack functional, membrane localized pre-TCR and TCR [4,19–22]. Moreover, a subset of T-ALLs can sustain loss of LCK and proliferate well in culture

[23–25], leading many to question the role of LCK and subsequent downstream TCR phosphorylation signaling as a driver of T-ALL survival and growth. By contrast, others have shown that glucocorticoid-resistant T-ALLs have high activity of LCK and yet high TCR signaling also kills T-ALL cells[26–28]. Taken together, these seemingly opposing roles of the TCR/LCK signaling pathway in T-ALL have confused the field for decades.

Here, we identified dasatinib and temsirolimus as a potent combination therapy for the treatment of a wide array of human T-ALL, including dexamethasone-resistant disease. Dasatinib inhibits LCK and subsequently the downstream TCR signaling pathway. By contrast, temsirolimus blocks mTORC1, a well-known regulator of proliferation, stemness, and therapy resistance in T-ALL[8,10,12,13,29,30]. These two pathways converge on the regulation of the MCL1 anti-apoptotic gene. We also discovered an unexpected role of LCK in driving continued leukemia growth and suggest that, like maturation of normal T cells that undergo positive and negative selection, T-ALLs require just the right levels of downstream TCR signaling to sustain growth and survival.

METHODS

Ex vivo drug screening using transgenic zebrafish ALL

Creation of mosaic CG1-strain transgenic animals, monitoring for ALL onset, and cell transplantation was performed as described (MGH #2011N000127)[31]. The *lck:mMyc* and *lck:mCherry* transgenes used the 7.5kb zebrafish *lck* promoter (Addgene plasmid 58891). Zebrafish ALL cells were harvested, plated into 96-well plates, incubated for 72 hours with drugs and analyzed by CellTiter-Glo assay. IC50 values were assigned using the GraphPad Prism software (GraphPad, San Diego, CA, USA). Combination indexes were calculated using the non-

constant ratio method within the CalcuSyn software package (Biosoft, Cambridge, UK) and synergy assigned if CI was < 1.0.

Human cell culture and *in vitro* drug treatments

$1x10^4$ - $4x10^4$ human T-ALL cells were plated per well in a volume of 100µl culture media in 96-well plates. Drugs were administered at a log2 or log4 dilution series. Cells were incubated at 37°C, 5% CO_2 and cell viability/growth analyzed by CellTiter-Glo after 24 or 72 hours of treatment (Promega, Madison, WI, USA)). Combination indexes were calculated using the constant ratio method in the CalcuSyn software package. Cell cycle and proliferation were assessed by flow cytometry using the Click-It EdU Kit (Life Technologies, Carlsbad, CA, USA) and apoptosis using the Annexin V Apoptosis Detection Kit APC (eBioscience, San Diego, CA, USA). Western blot analysis and flow cytometry was complete essentially as described [27] with primary and secondary antibodies noted in the supplemental methods.

Mouse xenograft studies

Mouse xenografts used luciferase-labeled cell lines and PDX models engrafted by tail—vein injection and were approved under animal protocol MGH#2009-P-002756. Cell line engrafted mice were treated after 15 days of engraftment while PDXs were treated when animals contained ≥5% hCD45 positive cells in the peripheral blood. Dasatinib was orally administered (10mg/kg/day, 80 mM citrate buffer pH 3.1) [32] and temsirolimus 8 hours later by intraperitoneal injection (10mg/kg/day)[33]. Survival analyses used the Kaplan-Meier Log-rank (Mantel-Cox) test using the GraphPad Prism software.

At necropsy, marrow, spleen, and peripheral blood were analyzed for percent blasts and phospho-S6K and phospho-LCK expression by flow cytometry. A portion of the spleen was fixed in 4% paraformaldehyde for histopathological examination that included hematoxylin and eosin staining, TUNEL, and IHC for hCD45, pLCK (Y394) and pS6K (T389). The ratio of positively

stained cells to unstained cells was calculated automatically in ImageJ [34] from three separate areas of each spleen. Significance was calculated by Unpaired t-test.

Analysis of primary patient sample responses to combination therapy

Bone marrow and peripheral blood collection from patients was performed in accordance with the Declaration of Helsinki (Pirkanmaa Hospital District Ethical Committee, ETL code R13109 and ethical committee of Helsinki University Hospital, permits 239/13/03/00/2010 and 303/13/03/01/2011). Viably frozen mononuclear cells were suspended in 12.5% HS-5 conditioned media (CM) [35] and $5x10^3$ live cells were seeded with MultiFlow FX.RAD (BioTek, Winooski, WT, USA) into compound containing 384 well-plates (25µl). Cell viability was measured using CellTiter-Glo (Promega). Sensitivity scores (DSS) [36] and synergy scores were assigned using the CalcuSyn software. Combination indexes were assigned using the SynergyFinder 2.0, the Loewe and ZIP reference models[37].

Analysis of human T-ALL samples

Immunophenotype, TCR status, fusion genes, translocations, clinical features, T-ALL subtype, and mutational profiles of T-ALL cell lines were gathered from public databases (https://depmap.org and https://humantallcelllines.wordpress.com/) and the literature [38–42]. Raw RNA-seq data of human T-ALL cell lines were acquired from NCBI SRA repository using sra-toolkit (v2.8.2-1) (GSE103046, GSE148522 and NCBI BioProject PRJNA523380)[43–45].

Primary patient samples were whole exome (WES) and mRNA sequenced and analyzed essentially as described[46–48]. Whole genome sequencing, WES and RNA-seq data of T-ALL patient samples are available in European Genome-phenome Archive under the accession number EGAS00001005945 or in OSFHOME with doi identifier 10.17605/OSF.IO/BK54U. Additional methods as supplemental material.

RESULTS

Ex vivo screening identifies combination therapies that kill zebrafish T-ALL

To rapidly identify drug sensitivities in T- and B-ALL, we developed an *ex vivo* screening platform to assess drug-induced cell killing of zebrafish ALL (Figure 1A). The zebrafish ALL model has identified genetic pathways that drive cancer progression [8,49–52] and have aided in developing therapeutic strategies for human disease[8,53–55]. The *rag2:mMyc* zebrafish model produces T-, B- and mixed lineage leukemias [56–59], while the new *lck:mMyc* transgenic model only develops CD4+/CD8+ clonal T-ALL (Supplementary Figure 1). Leukemia cells were harvested from *rag2:mMyc* and *lck:mMyc* ALL, plated into 96-well plates ($1x10^4$ cells/well, purity >90%), grown for 32 hours at 28.5ºC, treated with DMSO or compounds for 72 hours, and assessed for viability using CellTiter-Glo (Figure 1A). In total, 6 primary and 11 transplanted T-ALLs and 3 transplanted B-ALLs were assessed in the screen (Figures 1B). Ten FDA-approved and investigational drugs were assessed singly for effects on killing zebrafish ALL, including drugs commonly used as frontline and maintenance therapy including corticosteroids dexamethasone and prednisolone, and common chemotherapy agents like vincristine, doxorubicin, and L-asparaginase and small molecules such as AKT inhibitor MK-2206 and the general tyrosine kinase inhibitor dasatinib. As may be expected, our screening approach revealed wide differences in ALL drug sensitivities and varied leukemia responses to single drugs (Figure. 1B-C and Supplemental Figure 2). In total, seven of the ten drugs killed T-ALL cells from at least one model, with the most robust responses observed with glucocorticoids and MK-2206 (Figure 1B-C). Interestingly, primary *lck:mMyc* leukemia #1 (denoted with orange triangle) and *rag2:mMyc* leukemia #9 (denoted with blue triangle) were initially killed by dexamethasone and MK-2206, but their corresponding transplanted ALLs were resistant to these drugs (orange and blue circles, respectively, Figure 1B). Similarly, transplanted T-ALLs arising from the same primary leukemia #8 (denoted with green circles) also exhibited differing therapy responses between engrafted

leukemia clones. These results are consistent with both xenograft and zebrafish transplant experiments that show refractory T-ALL clones that drive relapse are selected following transplant and the extent to which clonal heterogeneity can drive therapy responses[8,11].

Given the potent single agent efficacy of dexamethasone, MK-2206, and dasatinib in killing a subset of zebrafish ALLs, we next assessed the pairwise combinations of each of these therapies in killing ALL using our *ex vivo* screening platform. Marked synergies were seen for each of these combinations (Figure 1B, D-E) and was expected for dexamethasone and MK-2206 or dasatinib and dexamethasone combination therapies that had been reported previously [8,13,26,60]. The most synergistic combination, dasatinib and MK-2206 ($CI_{Average}$ = 0.10) was novel (Figure 1D-E) and had not been previously investigated in the context of T-ALL. Importantly, many samples did not respond to single dasatinib or MK-2206 treatment but were exquisitely sensitive to combination therapy (Figure 1B). In total, four of nine dexamethasone-resistant zebrafish T-ALLs were effectively killed following combination treatment with dasatinib and MK-2206. Our data validates the utility of the high-throughput drug screening approach to identify potential new drug combinations for T-ALL, including dexamethasone-resistant leukemias.

Combination of dasatinib and AKT/mTOR inhibitors kill human T-ALL cells

We next assessed the efficiency of the combination of dasatinib and MK-2206 in human T-ALL, uncovering potent synergies of these drugs in killing Jurkat, MOLT-4 and PF-382 cells (Supplemental Figure 3). Neither drug alone was able to efficiently kill any of these T-ALL models. MK-2206 has adverse effects in patients and is not used clinically; thus, we repeated our drug combination experiments using dasatinib along with the clinically-available mTORC1 inhibitor temsirolimus in a larger panel of human T-ALL cell lines (Figure 2 and Supplemental Figure 4). Strong drug synergy in killing T-ALL was seen in five of 11 cell line models and included Jurkat, MOLT-4, PF-382, SUPT1 and DND41. This drug synergy was associated with elevated apoptosis and S-phase arrest (Figure 2). The remaining six non-synergistic T-ALL cell lines

exhibited heterogeneity in responses similar to those found in zebrafish T-ALL (Supplemental Figure 4B). There is an ongoing phase I clinical trial in children that complexes dasatinib and temsirolimus in advanced malignant solid tumors (NCT02389309), making this combination our top choice for prioritizing for further studies outlined below. These results show that co-targeting the AKT/mTOR pathway along with dasatinib leads to potent and synergistic cell killing in a large subset of human T-ALL by stalling the cell cycle and subsequently inducing cell death.

LCK mediates the effect of dasatinib

Because dasatinib is a potent inhibitor of the LCK kinase in normal T cells and Chimeric Antigen Receptor T cells (CAR T) [61–63] and LCK is required for TCR signaling [17,64,65], we next correlated the suppressed activity of the TCR/LCK pathway following combination treatment with dasatinib and either temsirolimus or MK-2206 (Figure 3A,B and Supplemental Figure 3D). Dasatinib alone or in combination elicited potent suppression of LCK phosphorylation at the activating phospho-tyrosine Y394 in Jurkat, MOLT-4 and PF-382 cells. This led to the inhibition of many downstream components of the TCR signaling pathway, including loss of phosphorylation of ZAP70 and LAT, both of which are required downstream of LCK for efficient signaling. By contrast, neither temsirolimus nor MK-2206 treatment had any effect on LCK phosphorylation or subsequent downstream TCR signaling molecules, but instead effectively inhibited the phosphorylation of S6K at residue Y389. Dasatinib treatment also partially decreased AKT phosphorylation which is in line with inhibition of the costimulatory CD28 receptor that elicits low-level crosstalk from LCK to the PI3K pathway but had little effect on phosphorylation of S6K. Our results show that dasatinib treatment results in inhibition of downstream TCR signaling and strongly suggest that LCK kinase is the target of dasatinib in T-ALL.

To directly test if LCK is the target of dasatinib, we next assessed drug effects in LCK-deficient Jurkat (J.Cam1.6) and three independent CRISPR-Cas9 edited LCK-null MOLT4 clones (Figure 3C,D and Supplemental Figure 5). As expected, LCK knockout cells were efficiently killed

by single treatment with MK-2206 AKT-inhibitor or temsirolimus mTOR-inhibitor (IC50 values provided in Supplemental Table 1). LCK-null cells exhibited strong sensitization to single agent temsirolimus but lacked synergy when complexed with dasatinib (Figures 3D and Supplemental Figure 5). ZAP70 is a kinase required for TCR pathway activity and is a downstream target of LCK. Thus, not surprisingly, ZAP70 deficient Jurkat (P116) cells were also exquisitely sensitive to MK2206 or temsirolimus mono-therapy and exhibited complete abrogation of synergy with dasatinib (Figure 3D). LCK phosphorylation was attenuated by dasatinib in ZAP70-deficient T-ALL cells without altering cell viability (Figures 3D and Supplemental Figure 5). These results indicate that dasatinib specifically inhibits the LCK signaling pathway and when complexed with inhibitors of AKT/mTOR pathway, potently kills human T-ALL.

Leukemic cells often suppress pro-apoptotic pathways as a mechanism for transformation and continued tumor maintenance[66–68]. In both T-ALL and normal T cell development, the antiapoptotic BCL-2 family of proteins are often upregulated to curb cell death [69,70] and include specific regulation of BCL-2, BCL-xL and MCL-1. Hence, we examined their expression in T-ALL cell lines in response to mono- and combination therapies (Figure 4A). Although dasatinib mono-therapy reduced BCL2 expression in MOLT4 and PF382 cells, and subsequently the phosphorylation of BCL2 (S70), which is required for the full anti-apoptotic function of BCL2[71], similar responses were not observed in Jurkat cells (Figure 4A). Moreover, down regulation of BCL2 was not further potentiated by single or co-treatment with temsirolimus, suggesting that BCL-2 down-regulation was not responsible for combination therapy-induced T-ALL cell killing. Expression of BCL-xL was not altered by single or combination therapies. By contrast, all three synergistic T-ALL cell lines potently suppressed MCL-1 protein expression following combination therapy. As would be predicted, if the TCR/LCK and mTORC1 pathways act in parallel and yet redundantly suppress apoptosis, single drug treatment with either temsirolimus or dasatinib had no impact on MCL1 expression in these models. Strikingly, CCRF-CEM and HPB-ALL cell lines that are not killed by combination dasatinib and temsirolimus also failed to downregulate MCL-1

protein expression following treatment (Supplemental Figure 6C). These data again suggest that MCL-1 is the convergent downstream target of LCK and mTORC1 pathways in combination responsive cell lines and supports a model by which non-responsive cell lines likely activate other pathways to maintain high levels of MCL-1 to support survival and growth. Finally, treatment with two MCL-1 inhibitors, AZD5991 and AMG-176, potently induced T-ALL cell killing in Jurkat, MOLT-4, and PF-382 cells which was not further increased by addition of either dasatinib or temsirolimus (Figure 4B and C and Supplemental Figure 6 A and B). These results are in keeping with potent responses of human T-ALL to MCL-1 monotherapy [54,72] and lack of cell death in T-ALL cells treated with BCL2 inhibitor alone[54,73,74]. These data again support a model where drug combination of dasatinib and temsirolimus converges on MCL1 to downregulate its expression and potentiate cell death in a subset of human T-ALLs.

Dasatinib and temsirolimus kill human T-ALL in mouse xenografts

To provide preclinical rationale for assessing temsirolimus and dasatinib combination therapy in patients, we next extended our analysis of therapy responses to PDX models and primary patient samples. Specifically, NOD/SCID/Il2gr-null mice (NSG) mice were engrafted with four PDX models and allowed to progress to have a high leukemia burden. T-ALL cells were isolated from the spleen and submitted to *ex vivo* drug testing. Following 72 hours of combination treatment, PDX T-ALL cells had reduced cell viability when assessed by CellTiter-Glo assay (Figure 5A), while single drug treatments had little effect. Importantly, all four PDX explant models responded to the combination therapy. Combination treatment resulted in diminished LCK and S6K phosphorylation in T-ALL cells following 30 minutes (S42512 and TA10) or 24 hours of drug treatment (24836 and 44179, Figure 5B), confirming on target drug responses in PDX explant cultures.

We next analyzed therapy responses from nine pediatric and five adult T-ALL diagnostic samples (Supplemental Table 2 and Figure 5C,D). Following *ex vivo* treatment, four primary

pediatric T-ALLs responded to combination therapy, one of which was resistant to dexamethasone-induced cell killing (ALLT-323, Figure 5C,D). By contrast, none of the adult T-ALLs tested showed similar responses to combination therapy. From analysis of drug responses in cell line models, patient-derived xenografts, and patient samples, we find that 45% of T-ALLs tested exhibited synergistic killing following combination dasatinib and temsirolimus treatment (n=13 out of 29, Supplemental Figure 7C). Analysis of responses across T-ALL subtypes and association with specific genetic mutations failed to identify any obvious biomarkers or correlations in predicting therapy responses (Supplemental Figure 7 and Supplemental Table 2), although there appeared to be a trend toward higher TCR/LCK pathway activity in samples that exhibited synergistic therapy responses (Supplemental Figure 7B). These results are akin to those recently described in predicting transient dasatinib monotherapy responses in human T-ALL based on high TCR signaling component expression[60].

We next assessed the *in vivo* efficacy of these drugs using mouse xenograft models. First, MOLT-4 and Jurkat cells were lentiviral transfected with a luciferase/dsRED2 reporter and engrafted into immune deficient NOD/SCID/Il2gr-null (NSG) mice by tail-vein intravenous injection. Once animals developed systemic disease by 15 days post engraftment, mice were randomized into vehicle control, single drug treatment, or combination treatment groups. As expected, vehicle-treated animals exhibited progressive disease that was associated with increased leukemia burden and resulted in early morbidity (Figure 6A-D and Supplemental Figure 8A-C). Single-drug treatment also failed to efficiently curb human T-ALL growth *in vivo*. By contrast, combination therapy potently inhibited growth of both Jurkat and MOLT-4 leukemias grown in NSG mice. Mice treated with the drug combination also had reduced numbers of T-ALL cells in peripheral blood, bone marrow and spleen after extended drug treatment (Figure 6E and Supplemental Figure 8D). Flow cytometry also confirmed on-target inhibitory activity of dasatinib and temsirolimus in curbing pLCK and pS6K in human T-ALL cells obtained from the peripheral blood, bone marrow and spleen of engrafted mice (Supplemental Figure 8E). Histopathological

staining confirmed overall increases in apoptotic lymphoblasts in the spleen following combination therapy in both MOLT-4 and Jurkat engrafted animals at the end of treatment (Figure 6F,G and Supplemental Figure 8F). Immunohistochemistry also confirmed a decrease of CD45+ cells in combination treated spleens and an overall diminution of fluorescence intensity for pS6K and pLCK in combination treated CD45+ T-ALL cells (Figures 6F,H and Supplemental Figure 9).

To validate the drug combination efficacy in killing patient-derived xenografts as the highest standard for preclinical evaluation, we next engrafted two PDXs into immunodeficient NOD/SCID/Il2gr-null (NSG) mice by intravenous tail-vein injection (Fig. 7A, PDX 44179 and PDX 24836). Animals were treated when $\geq$5% leukemic blasts were detected in the circulating blood by 15-20 days post-engraftment. Mice were then randomized into treatment groups and treated for 8 weeks. Blood was analyzed weekly by cheek bleeds and the amount of leukemia blasts were measured by flow cytometry and quantified as the percentage of human CD45 positive cells present in blood circulation (Figure 7A). Vehicle and mono-therapy treated mice exhibited rapid leukemia onset with high leukemia burden, whereas mice treated with the combination therapy had lower circulating leukemic blasts being found throughout the treatment (Figure 7B,C,G,H). Flow cytometry also confirmed that combination treated animals had lower percentages of CD45+ leukemic blasts in the peripheral blood, bone marrow and spleen at the end of treatment, even when compared with mono-therapy treated mice (Figure 7D,I). TUNEL staining confirmed overall increases in apoptotic lymphoblasts in the spleen following combination therapy in both PDX models (Figures 7E,J and Supplemental Figure 10). We also confirmed on-target efficiency of temsirolimus and dasatinib by observing a diminution of fluorescence intensity of pS6K and pLCK in CD45+ T-ALL cells found in the spleen (Figure 7F,K and Supplemental Figure 10). There were no adverse effects on overall health, survival and average body weight between leukemic mice treated with control, single- or double-drug combination over the course of treatment (Supplemental Figure 9B), suggesting that the drug combination was well-tolerated in mice.

These data confirm that dasatinib and temsirolimus kill a subset of patient-derived human T-ALL *in vivo.*

DISCUSSION

We have identified that dasatinib suppresses LCK kinase activation and subsequently turns off the TCR signaling pathway to halt cell cycle progression and induce T-ALL cell death. Since T-ALL cells often lack functional TCR [75] and LCK-deficient T-ALL cell lines are viable [23], the role of LCK as a critical driver of T-ALL viability was unexpected. We and others have recently identified the exquisite dependency of T-ALL cells on achieving the right balance of TCR signaling to sustain growth. For example, Trinquand *et al.* showed that hyperactive TCR signaling kills T-ALL cells [28] while we uncovered that the PRL3 phosphatase suppresses hyperactive T-cell phosphorylation signaling pathways to suppress apoptosis in leukemia cells[27]. The results presented here starkly contrast with these studies and rather suggest a Goldilocks scenario where LCK and downstream TCR signaling must be sustained and fine-tuned to stimulate leukemia cell growth. Our data, along with others[60,76], supports a model where dasatinib inhibits LCK function by blocking downstream signals from the TCR signaling complex, leading to suppressed proliferation and death in a large fraction of T-ALL. Yet, the dependency of MOLT-4 and PF-382 cells on LCK signaling was unexpected, as these cells lack intact and functional TCR[75,77]. As recently suggested by our group[27], downstream phosphorylation of classic TCR signaling molecules can be regulated in a receptor agnostic manner in T-ALL and likely represents a new therapeutic vulnerability for a substantial fraction of human T-ALLs. These data raise the intriguing hypothesis that other tyrosine kinase receptors or downstream mutational activation of TCR pathway components activate LCK in a subset of T-ALL to drive continued leukemia growth and will surely be the subject of future studies.

Our work also uncovered potent drug synergies between dasatinib and temsirolimus in killing a subset of human T-ALL and specifically targeting LCK and S6K phosphorylation, respectively. Dasatinib and other tyrosine kinase inhibitors have been utilized for the treatment of Philadelphia chromosome positive B-ALL, NUP214-ABL1+ T-ALL and ABL1 amplified T-ALL [78], suggesting the utility and well-tolerated application of dasatinib in the clinic. Yet, single drug treatment often leads to the acquisition of dasatinib-resistant mutations within the BCR-ABL1 kinase domain [79] or the compensatory upregulation of Shp2/Ras/ERK and PI3K/AKT/mTOR pathways[80]. Similar results were recently extended to non-ABL1 rearranged human T-ALL, where dasatinib mono-therapy lead to only short-term responses in killing human T-ALL *in vivo* with a large majority of leukemias rapidly progressing on mono-therapy[60,81]. Additionally, a case report of one refractory T-ALL patient treated with dasatinib monotherapy reported a relapse after few months of treatment[82]. In the context of chronic myeloid leukemia (CML), the dual PI3K/mTOR inhibitor NVP-BEZ235 re-sensitized resistant cells to TKI treatment and induced potent cell killing[80]. These data suggest that ABL kinase and mTORC1 lie in the same linear pathway to drive sustained tumor growth in CML. By contrast, our work in T-ALL has uncovered that the TCR/LCK signaling pathway and AKT/mTORC1 largely function in parallel and redundant pathways to inhibit apoptosis and sustain growth by in part by modulating MCL-1 expression. In the setting of T-ALL, MCL-1 protein stability is regulated in part by TCR signaling and acts independent of transcriptional changes in *MCL1* [83,84]*.* MCL-1 protein stability is also regulated by growth factors, PI3K, and AKT in wide array of cancers, including human T-ALL[85]. For example, chemical epistasis experiments have shown that PI3K inhibition regulates MCL-1 phosphorylation on S159 through a GSK-dependent mechanism, resulting in ubiquitination and proteasomal degradation in human T-ALL[72,86] . Future studies will focus on uncovering the precise mechanisms by which each pathway regulates MCL1 expression in T-ALL.

Combination of dasatinib and temsirolimus therapy killed 45% of human T-ALLs tested, was agnostic of T-ALL subtype or mutational spectrum, and killed dexamethasone-refractory

zebrafish and human T-ALL. This drug combination was well tolerated over the 8-weeks of treatment with no adverse effects, animal losses, or significant changes in weight across all four models tested to date. Indeed, combination of dasatinib and everolimus, an mTOR inhibitor related to temsirolimus with similar in function, was recently evaluated in high-grade pediatric glioma patients and had limited toxicity that included rash, mucositis, and fatigue that did not require dose reduction. No significant adverse events reported[87]. In total, our work now provides *in vivo* pre-clinical validation for combination of dasatinib and temsirolimus for treatment of aggressive and therapy resistant T-ALL that will be likely useful for a large fraction of patients.

Finally, we demonstrate that co-administration of dasatinib and AKT/mTORC1 pathway inhibitors synergize to kill human T-ALL, likely in part, by the convergent downregulation of the MCL-1, an anti-apoptotic protein of the Bcl-2 family. Indeed MCL-1 is translationally upregulated by the mTORC1 pathway in B-cell lymphomas and is regulated at multiple stages of T cell maturation and following LCK/TCR pathway activation[83,88]. Interestingly, MCL-1 dependency is seen in a wide array of hematological and solid malignancies, including T-ALL[54,72,89,90]. However, direct targeting of MCL-1 as a monotherapy in hematological malignancies results in serious side effects including cardiac toxicity[91]. Moreover, MCL1 loss in mouse models results in severe hematologic defects [92,93], impaired neural development [94], and defects in synovial fibroblasts [95] suggesting a low-therapeutic window for the use of MCL-1 inhibitors in the setting of pediatric cancers. Rather, reducing MCL1 expression by targeting tissue-restricted pathways like TCR signaling along with mTORC1 may provide better and more tractable therapeutic strategy to deploy clinically in T-ALL.

Ultimately, our studies provided new insights into LCK-mediated signaling effects on T-ALL survival and credential dasatinib and temsirolimus as a new combination therapy for killing pediatric T-ALL that should be considered for future clinical evaluation.

Author contributions: D.L., O.L., S.L. and A.V. conceived the study, S.L., A.V., C.Y., L.O., D.D, A.H.J., E.J.A., L.W., J.R.A., K.M., A.A. and N.H. conducted experiments, S. Lo. and J.Y. produced gateway plasmids, S.I, S.M, S.A and S.P.G. analyzed sequencing data, C.Y., K.G. and M.K. advised in animal experiments, A.P. assisted with primary patient samples, T.R. advised with the experimental design and data analysis of primary patient samples, C.A.H. provided primary patient samples and advised with the data, M.H. advised with data, D.L. and O.L. supervised the study. All authors reviewed and accepted the manuscript.

Acknowledgement: We want to acknowledge Finnish IT center for science and UEF Bioinformatics Center, University of Eastern Finland, Finland, for computation resources. We also wish to thank Eini Eskola for assistance in laboratory work. Furthermore, we want to thank Dr. David Weinstock for kindly providing PDX samples, Dr. Tony Letai for advice on apoptotic pathways to analyze in treated T-ALLs, and Dr. Brian Millet and Daniel O'Neill for thoughtful discussions. We are grateful to the patients for providing samples for our studies. The FIMM Technology Center High Throughput Biomedicine Unit and Sequencing Lab are acknowledged for their expert technical support.

Financial support: This work was supported by NIH grant R01CA211734 (D.M.L), the MGH Research Scholar Award (D.M.L.), Academy of Finland (O.L. and M.H. 321553, O.L., 310106), Cancer Foundation Finland (O.L., M.H., C.A.H), Jane and Aatos Erkko Foundation (O.L., M.H.), Sigrid Juselius Foundation (O.L., M.H., C.A.H), Aamu Foundation (O.L.), Finnish Hematology Association (S.L.), Finnish Blood Disease Research Foundation (S.L.), and the Competitive State Research Financing of the Expert Responsibility Area of Tampere University Hospital (O.L. 9V033 and 9X027). FIMM High Throughput Biomedicine Unit and Sequencing Lab are financially supported by the University of Helsinki (HiLife) and Biocenter Finland.

Conflict of interest disclosure statement: C.A.H. has received research funding from Celgene, KronosBio, Novartis, Oncopeptides, Orion Pharma, and the IMI2 projects HARMONY and HARMONY PLUS unrelated to this study.

REFERENCES

1. Hao T, Li-Talley M, Buck A, Chen WY. An emerging trend of rapid increase of leukemia but not all cancers in the aging population in the United States. *Sci. Rep.* 2019;9(1):.

2. Van Vlierberghe P, Ferrando A. The molecular basis of T cell acute lymphoblastic leukemia. *J. Clin. Invest.* 2012;122(10):3398–3406.

3. Girardi T, Vicente C, Cools J, De Keersmaecker K. The genetics and molecular biology of T-ALL. *Blood*. 2017;129(9):1113–1123.

4. Tremblay CS, Hoang T, Hoang T. Early T cell differentiation lessons from T-cell acute lymphoblastic leukemia. *Prog. Mol. Biol. Transl. Sci.* 2010;92(C):121–156.

5. Gutierrez A, Sanda T, Grebliunaite R, et al. High frequency of PTEN, PI3K, and AKT abnormalities in T-cell acute lymphoblastic leukemia. *Blood*. 2009;114(3):647–650.

6. Lonetti A, Cappellini A, Bertaina A, et al. Improving nelarabine efficacy in T cell acute lymphoblastic leukemia by targeting aberrant PI3K/AKT/mTOR signaling pathway. *J. Hematol. Oncol.* 2016;9(1):1–16.

7. Lynch JT, McEwen R, Crafter C, et al. Identification of differential PI3K pathway target dependencies in T-cell acute lymphoblastic leukemia through a large cancer cell panel screen. *Oncotarget*. 2016;7(16):22128–22139.

8. Blackburn JS, Liu S, Wilder JL, et al. Clonal evolution enhances leukemia-propagating cell frequency in T cell acute lymphoblastic leukemia through Akt/mTORC1 pathway activation. *Cancer Cell*. 2014;25(3):366–378.

9. Liu Y, Easton J, Shao Y, et al. The genomic landscape of pediatric and young adult T-lineage acute lymphoblastic leukemia. *Nat. Genet.* 2017;49(8):1211–1218.

10. De Smedt R, Morscio J, Goossens S, Van Vlierberghe P. Targeting steroid resistance in T-cell acute lymphoblastic leukemia. *Blood Rev.* 2019;38:.

11. Clappier E, Gerby B, Sigaux F, et al. Clonal selection in xenografted human T cell acute lymphoblastic leukemia recapitulates gain of malignancy at relapse. *J. Exp. Med.* 2011;208(4):653–661.

12. Cantley AM, Welsch M, Ambesi-Impiombato A, et al. Small Molecule that Reverses Dexamethasone Resistance in T-cell Acute Lymphoblastic Leukemia (T-ALL). *ACS Med. Chem. Lett.* 2014;5(7):754–759.

13. Piovan E, Yu J, Tosello V, et al. Direct reversal of glucocorticoid resistance by AKT inhibition in acute lymphoblastic leukemia. *Cancer Cell*. 2013;24(6):766–776.

14. Chiang YJ, Hodes RJ. T-cell development is regulated by the coordinated function of proximal and distal Lck promoters active at different developmental stages. *Eur. J. Immunol.* 2016;46(10):2401–2408.

15. Palacios EH, Weiss A. Function of the Src-family kinases, Lck and Fyn, in T-cell development and activation. *Oncogene 2004 2348*. 2004;23(48):7990–8000.

16. Van Oers NSC, Lowin-Kropf B, Finlay D, Connolly K, Weiss A. alpha beta T cell development is abolished in mice lacking both Lck and Fyn protein tyrosine kinases. *Immunity*. 1996;5(5):429–436.

17. Gascoigne NRJ, Casas J, Brzostek J, Rybakin V. Initiation of TCR Phosphorylation and Signal Transduction. *Front. Immunol.* 2011;2:72.

18. Love PE, Hayes SM. ITAM-mediated signaling by the T-cell antigen receptor. *Cold Spring Harb. Perspect. Biol.* 2010;2(6):.

19. Cordo' V, van der Zwet JCG, Canté-Barrett K, Pieters R, Meijerink JPP. T-cell Acute Lymphoblastic Leukemia: A Roadmap to Targeted Therapies. *Blood cancer Discov.* 2020;2(1):19–31.

20. van Dongen JJ, Krissansen GW, Wolvers-Tettero IL, et al. Cytoplasmic expression of the CD3 antigen as a diagnostic marker for immature T-cell malignancies. *Blood*. 1988;71(3):603–612.

21. Gocho Y, Yang JJ. Genetic defects in hematopoietic transcription factors and predisposition to acute lymphoblastic leukemia. *Blood*. 2019;134(10):793–797.

22. Cordo' V, Meijer MT, Hagelaar R, et al. Phosphoproteomic profiling of T cell acute lymphoblastic leukemia reveals targetable kinases and combination treatment strategies. *Nat. Commun. 2022 131*. 2022;13(1):1–13.

23. Goldsmith MA, Weiss A. Isolation and characterization of a T-lymphocyte somatic mutant with altered signal transduction by the antigen receptor. *Proc. Natl. Acad. Sci. U. S. A.* 1987;84(19):6879–6883.

24. Straus DB, Weiss A. Genetic evidence for the involvement of the lck tyrosine kinase in signal transduction through the T cell antigen receptor. *Cell*. 1992;70(4):585–593.

25. Vico-Barranco I, Arbulo-Echevarria MM, Serrano-García I, et al. A Novel, LAT/Lck Double Deficient T Cell Subline J.CaM1.7 for Combined Analysis of Early TCR Signaling. *Cells*. 2021;10(2):1–20.

26. Serafin V, Capuzzo G, Milani G, et al. Glucocorticoid resistance is reverted by LCK inhibition in pediatric T-cell acute lymphoblastic leukemia. *Blood*. 2017;130(25):2750–2761.

27. Garcia EG, Veloso A, Oliveira ML, et al. PRL3 enhances T-cell acute lymphoblastic leukemia growth through suppressing T-cell signaling pathways and apoptosis. *Leuk. 2020 353*. 2020;35(3):679–690.

28. Trinquand A, Dos Santos NR, Quang CT, et al. Triggering the TCR Developmental Checkpoint Activates a Therapeutically Targetable Tumor Suppressive Pathway in T-cell Leukemia. *Cancer Discov.* 2016;6(9):973–985.

29. Evangelisti C, Chiarini F, McCubrey JA, Martelli AM. Therapeutic Targeting of mTOR in T-Cell Acute Lymphoblastic Leukemia: An Update. *Int. J. Mol. Sci.* 2018;19(7):.

30. Rheingold SR, Tasian SK, Whitlock JA, et al. A Phase 1 trial of temsirolimus and intensive re-induction chemotherapy for 2nd or greater relapse of acute lymphoblastic leukaemia: a Children's Oncology Group study (ADVL1114). *Br. J. Haematol.* 2017;177(3):467.

31. Blackburn JS, Liu S, Langenau DM. Quantifying the frequency of tumor-propagating cells using limiting dilution cell transplantation in syngeneic zebrafish. *J. Vis. Exp.* 2011;(53):.

32. Boulos N, Mulder HL, Calabrese CR, et al. Chemotherapeutic agents circumvent emergence of dasatinib-resistant BCR-ABL kinase mutations in a precise mouse model of Philadelphia chromosome-positive acute lymphoblastic leukemia. *Blood*. 2011;117(13):3585–3595.

33. Teachey DT, Obzut DA, Cooperman J, et al. The mTOR inhibitor CCI-779 induces apoptosis and inhibits growth in preclinical models of primary adult human ALL. *Blood*. 2006;107(3):1149–1155.

34. Schneider CA, Rasband WS, Eliceiri KW. NIH Image to ImageJ: 25 years of image analysis. *Nat. Methods 2012 97*. 2012;9(7):671–675.

35. Karjalainen R, Pemovska T, Popa M, et al. JAK1/2 and BCL2 inhibitors synergize to counteract bone marrow stromal cell-induced protection of AML. *Blood*. 2017;130(6):789–802.

36. Yadav B, Pemovska T, Szwajda A, et al. Quantitative scoring of differential drug sensitivity for individually optimized anticancer therapies. *Sci. Reports 2014 41*. 2014;4(1):1–10.

37. Ianevski A, Giri AK, Aittokallio T. SynergyFinder 2.0: visual analytics of multi-drug combination synergies. *Nucleic Acids Res.* 2020;48(W1):W488–W493.

38. Nagel S, Venturini L, Meyer C, et al. Multiple mechanisms induce ectopic expression of LYL1 in subsets of T-ALL cell lines. *Leuk. Res.* 2010;34(4):521–528.

39. Atak ZK, de Keersmaecker K, Gianfelici V, et al. High Accuracy Mutation Detection in Leukemia on a Selected Panel of Cancer Genes. *PLoS One*. 2012;7(6):e38463.

40. Elwood NJ, Green AR, Melder A, Begley CG, Nicola N. The SCL protein displays cell-specific heterogeneity in size. *Leukemia*. 1994;8(1):106–114.

41. Drexler HG. The leukemia-lymphoma cell line factsbook. 2000;

42. Mansour MR, Abraham BJ, Anders L, et al. Oncogene regulation. An oncogenic super-enhancer formed through somatic mutation of a noncoding intergenic element. *Science*. 2014;346(6215):1373–1377.

43. Ngoc PCT, Tan SH, Tan TK, et al. Identification of novel lncRNAs regulated by the TAL1 complex in T-cell acute lymphoblastic leukemia. *Leukemia*. 2018;32(10):2138–2151.

44. Shaw TI, Dong L, Tian L, et al. Integrative network analysis reveals USP7 haploinsufficiency inhibits E-protein activity in pediatric T-lineage acute lymphoblastic leukemia (T-ALL). *Sci. Reports 2021 111*. 2021;11(1):1–12.

45. Ghandi M, Huang FW, Jané-Valbuena J, et al. Next-generation characterization of the Cancer Cell Line Encyclopedia. *Nat. 2019 5697757*. 2019;569(7757):503–508.

46. Koskela HLM, Eldfors S, Ellonen P, et al. Somatic STAT3 mutations in large granular lymphocytic leukemia. *N. Engl. J. Med.* 2012;366(20):1905–1913.

47. Dufva O, Pölönen P, Brück O, et al. Immunogenomic Landscape of Hematological Malignancies. *Cancer Cell*. 2020;38(3):424–428.

48. Laukkanen S, Oksa L, Nikkilä A, et al. SIX6 is a TAL1-regulated transcription factor in T-ALL and associated with inferior outcome. *Leuk. Lymphoma*. 2020;61(13):3089–3100.

49. Blackburn JS, Liu S, Raiser DM, et al. Notch signaling expands a pre-malignant pool of T-cell acute lymphoblastic leukemia clones without affecting leukemia-propagating cell frequency. *Leukemia*. 2012;26(9):2069–2078.

50. Lobbardi R, Pinder J, Martinez-Pastor B, et al. TOX Regulates Growth, DNA Repair, and Genomic Instability in T-cell Acute Lymphoblastic Leukemia. *Cancer Discov.* 2017;7(11):1336–1353.

51. Feng H, Stachura DL, White RM, et al. T-Lymphoblastic Lymphoma Cells Express High Levels of BCL2, S1P1 and ICAM1 Leading to a Blockade of Tumor Cell Intravasation. *Cancer Cell*. 2010;18(4):353.

52. Mansour MR, He S, Li Z, et al. JDP2: An oncogenic bZIP transcription factor in T cell acute lymphoblastic leukemia. *J. Exp. Med.* 2018;215(7):1929–1945.

53. Ridges S, Heaton WL, Joshi D, et al. Zebrafish screen identifies novel compound with selective toxicity against leukemia. *Blood*. 2012;119(24):5621–5631.

54. Li Z, He S, Look AT. The MCL1-specific inhibitor S63845 acts synergistically with venetoclax/ABT-199 to induce apoptosis in T-cell acute lymphoblastic leukemia cells. *Leukemia*. 2019;33(1):262–266.

55. Gutierrez A, Pan L, Groen RWJ, et al. Phenothiazines induce PP2A-mediated apoptosis in T cell acute lymphoblastic leukemia. *J. Clin. Invest.* 2014;124(2):644–655.

56. Garcia EG, Iyer S, Garcia SP, et al. Cell of origin dictates aggression and stem cell number in acute lymphoblastic leukemia. *Leukemia*. 2018;32(8):1860–1865.

57. Borga C, Foster CA, Iyer S, et al. Molecularly distinct models of zebrafish Myc-induced B cell leukemia. *Leukemia*. 2019;33(2):559–562.

58. Langenau DM, Traver D, Ferrando AA, et al. Myc-induced T cell leukemia in transgenic zebrafish. *Science*. 2003;299(5608):887–890.

59. Borga C, Park G, Foster C, et al. Simultaneous B and T cell acute lymphoblastic

leukemias in zebrafish driven by transgenic MYC: implications for oncogenesis and lymphopoiesis. *Leukemia*. 2019;33(2):333–347.

60. Gocho Y, Liu J, Hu J, et al. Network-based systems pharmacology reveals heterogeneity in LCK and BCL2 signaling and therapeutic sensitivity of T-cell acute lymphoblastic leukemia. *Nat. Cancer 2021 23*. 2021;2(3):284–299.

61. Schade AE, Schieven GL, Townsend R, et al. Dasatinib, a small-molecule protein tyrosine kinase inhibitor, inhibits T-cell activation and proliferation. *Blood*. 2008;111(3):1366.

62. Lee KC, Ouwehand I, Giannini AL, et al. Lck is a key target of imatinib and dasatinib in T-cell activation. *Leukemia*. 2010;24(4):896–900.

63. Suryadevara CM, Desai R, Harrison Farber S, et al. Preventing Lck Activation in CAR T Cells Confers Treg Resistance but Requires 4-1BB Signaling for Them to Persist and Treat Solid Tumors in Nonlymphodepleted Hosts. *Clin. Cancer Res.* 2019;25(1):358–368.

64. Rossy J, Williamson DJ, Gaus K. How does the kinase Lck phosphorylate the T cell receptor? Spatial organization as a regulatory mechanism. *Front. Immunol.* 2012;3:167.

65. Hwang JR, Byeon Y, Kim D, Park SG. Recent insights of T cell receptor-mediated signaling pathways for T cell activation and development. *Exp. Mol. Med.* 2020;52(5):750–761.

66. Prokop A, Wieder T, Sturm I, et al. Relapse in childhood acute lymphoblastic leukemia is associated with a decrease of the Bax/Bcl-2 ratio and loss of spontaneous caspase-3 processing in vivo. *Leukemia*. 2000;14(9):1606–1613.

67. Egle A, Harris AW, Bouillet P, Cory S. Bim is a suppressor of Myc-induced mouse B cell leukemia. *Proc. Natl. Acad. Sci. U. S. A.* 2004;101(16):6164–6169.

68. Bachmann PS, Piazza RG, Janes ME, et al. Epigenetic silencing of BIM in glucocorticoid poor-responsive pediatric acute lymphoblastic leukemia, and its reversal by histone deacetylase inhibition. *Blood*. 2010;116(16):3013–3022.

69. Gratiot-Deans J, Merino R, Nuñez G, Turka LA. Bcl-2 expression during T-cell development: early loss and late return occur at specific stages of commitment to differentiation and survival. *Proc. Natl. Acad. Sci. U. S. A.* 1994;91(22):10685.

70. Peirs S, Matthijssens F, Goossens S, et al. ABT-199 mediated inhibition of BCL-2 as a novel therapeutic strategy in T-cell acute lymphoblastic leukemia. *Blood*. 2014;124(25):3738–3747.

71. Ruvolo PP, Deng X, May WS. Phosphorylation of Bcl2 and regulation of apoptosis. *Leukemia*. 2001;15(4):515–522.

72. Inuzuka H, Shaik S, Onoyama I, et al. SCFFBW7 regulates cellular apoptosis by targeting MCL1 for ubiquitylation and destruction. *Nat. 2011 4717336*. 2011;471(7336):104–109.

73. Choudhary GS, Al-Harbi S, Mazumder S, et al. MCL-1 and BCL-xL-dependent resistance

to the BCL-2 inhibitor ABT-199 can be overcome by preventing PI3K/AKT/mTOR activation in lymphoid malignancies. *Cell Death Dis.* 2015;6(1):.

74. Suryani S, Carol H, Chonghaile TN i., et al. Cell and molecular determinants of in vivo efficacy of the BH3 mimetic ABT-263 against pediatric acute lymphoblastic leukemia xenografts. *Clin. Cancer Res.* 2014;20(17):4520–4531.

75. Hara J, Benedict SH, Champagne E, et al. Comparison of T cell receptor alpha, beta, and gamma gene rearrangement and expression in T cell acute lymphoblastic leukemia. *J. Clin. Invest.* 1988;81(4):989–996.

76. Laukkanen S, Grönroos T, Pölönen P, et al. In silico and preclinical drug screening identifies dasatinib as a targeted therapy for T-ALL. *Blood Cancer J. 2017 79*. 2017;7(9):e604–e604.

77. Sandberg Y, Verhaaf B, van Gastel-Mol EJ, et al. Human T-cell lines with well-defined T-cell receptor gene rearrangements as controls for the BIOMED-2 multiplex polymerase chain reaction tubes. *Leukemia*. 2007;21(2):230–237.

78. Crombet O, Lastrapes K, Zieske A, Morales-Arias J. Complete morphologic and molecular remission after introduction of dasatinib in the treatment of a pediatric patient with t-cell acute lymphoblastic leukemia and ABL1 amplification. *Pediatr. Blood Cancer*. 2012;59(2):333–334.

79. Soverini S, Colarossi S, Gnani A, et al. Resistance to dasatinib in Philadelphia-positive leukemia patients and the presence or the selection of mutations at residues 315 and 317 in the BCR-ABL kinase domain. *Haematologica*. 2007;92(3):401–404.

80. Wöhrle FU, Halbach S, Aumann K, et al. Gab2 signaling in chronic myeloid leukemia cells confers resistance to multiple Bcr-Abl inhibitors. *Leukemia*. 2013;27(1):118–129.

81. Shi Y, Beckett MC, Blair HJ, et al. Phase II-like murine trial identifies synergy between dexamethasone and dasatinib in T-cell acute lymphoblastic leukemia. *Haematologica*. 2021;106(4):1056–1066.

82. Frismantas V, Dobay MP, Rinaldi A, et al. Ex vivo drug response profiling detects recurrent sensitivity patterns in drug-resistant acute lymphoblastic leukemia. *Blood*. 2017;129(11):e26–e37.

83. Dzhagalov I, Dunkle A, He Y-W. The anti-apoptotic Bcl-2 family member Mcl-1 promotes T lymphocyte survival at multiple stages. *J. Immunol.* 2008;181(1):521–528.

84. Wensveen FM, van Gisbergen KPJM, Derks IAM, et al. Apoptosis threshold set by Noxa and Mcl-1 after T cell activation regulates competitive selection of high-affinity clones. *Immunity*. 2010;32(6):754–765.

85. Thomas LW, Lam C, Edwards SW. Mcl-1; the molecular regulation of protein function. *FEBS Lett.* 2010;584(14):2981–2989.

86. Maurer U, Charvet C, Wagman AS, Dejardin E, Green DR. Glycogen synthase kinase-3 regulates mitochondrial outer membrane permeabilization and apoptosis by

destabilization of MCL-1. *Mol. Cell*. 2006;21(6):749–760.

87. Miklja Z, Yadav VN, Cartaxo RT, et al. Everolimus improves the efficacy of dasatinib in PDGFRα-driven glioma. *J. Clin. Invest.* 2020;130(10):5313–5325.

88. Mills JR, Hippo Y, Robert F, et al. mTORC1 promotes survival through translational control of Mcl-1. *Proc. Natl. Acad. Sci. U. S. A.* 2008;105(31):10853–10858.

89. Campbell KJ, Mason SM, Winder ML, et al. Breast cancer dependence on MCL-1 is due to its canonical anti-apoptotic function. *Cell Death Differ. 2021 289*. 2021;28(9):2589–2600.

90. Nangia V, Siddiqui FM, Caenepeel S, et al. Exploiting MCL1 Dependency with Combination MEK + MCL1 Inhibitors Leads to Induction of Apoptosis and Tumor Regression in KRAS-Mutant Non-Small Cell Lung Cancer. *Cancer Discov.* 2018;8(12):1598–1613.

91. Roberts AW, Wei AH, Huang DCS. BCL2 and MCL1 inhibitors for hematologic malignancies. *Blood*. 2021;138(13):1120–1136.

92. Opferman JT, Letai A, Beard C, et al. Development and maintenance of B and T lymphocytes requires antiapoptotic MCL-1. *Nat. 2003 4266967*. 2003;426(6967):671–676.

93. Opferman JT, Iwasaki H, Ong CC, et al. Obligate role of anti-apoptotic MCL-1 in the survival of hematopoietic stem cells. *Science*. 2005;307(5712):1101–1104.

94. Arbour N, Vanderluit JL, Le Grand JN, et al. Mcl-1 Is a Key Regulator of Apoptosis during CNS Development and after DNA Damage. *J. Neurosci.* 2008;28(24):6068.

95. Liu H, Eksarko P, Temkin V, et al. Mcl-1 is essential for the survival of synovial fibroblasts in rheumatoid arthritis. *J. Immunol.* 2005;175(12):8337–8345.

FIGURE LEGENDS

Figure 1. *Ex vivo* drug screening identifies synergies between dasatinib and AKT inhibitor in killing dexamethasone-resistant zebrafish T-ALL. A) Schematic of experimental design. B) Comparison of single and combination drug responses in primary (triangles) and transplanted ALL (circles). T-ALL samples are denoted by filled shapes while B-ALL samples are represented as open shapes. Samples with the same color originate from the same primary leukemia (orange, blue, and green). C) Representative dose response curves for sensitive (solid line) and insensitive

ALLs (dotted line) to single drug treatment with dexamethasone (Dex), MK-2206, or dasatinib (Das). D) Dose response curves following single drug and combination therapy for a representative, transplanted *lck:cMyc* T-ALL (L1.5). Green line highlights synergistic drug combinations. E) Isobolograms normalized to the IC50 of each drug. Combination Index Average ($CI_{average}$) derived from all experimental data points with <1 indicating synergy. Error bars +/- SEM. n=3 samples/data point (C-E). *, $p < 0.05$; **, $p < 0.01$ by Student's two tailed t-test.

Figure 2. Combination of dasatinib and temsirolimus mTOR inhibitor elicit potent cell cycle arrest and leukemia cell killing in human T-ALL. A) Jurkat. B) MOLT-4. C) PF-382. Dose response curves following single drug and combination therapy (left panels). Dasatinib and temsirolimus after 72 hours of treatment and assessed by CellTiter-Glo. Combination indexes for ED50 concentrations are shown. Green lines highlight synergistic combination treatments. Cell proliferation assessed by EdU/PI staining (middle panels). Apoptosis assessed by AnnexinV/PI staining (right panels). Error bars +/- SEM. n=3 samples/data point. * $p < 0.05$, ** $p<0.01$, *** $p<0.001$ in comparing single vs. combination treated cells (left panels) or in assessing differences in overall percentages of cells in S-phase or AnnexinV+/PI+ cells by Student's two tailed t-test (middle and right panels).

Figure 3. Dasatinib inhibits LCK phosphorylation and downstream TCR signaling and induces cell killing when co-treated with temsirolimus. A) Schematic of T-cell receptor and PI3K/AKT/mTOR signaling pathways along with pathway inhibitors. B) Western blot analysis of T-ALL cells following drug treatment (dasatinib at 100nM, temsirolimus at 200nM) for 30 minutes. Representative blot from three biological replicates. C) Western blot showing expression of total LCK and ZAP70 in Jurkat and MOLT-4 wild-type, LCK deficient (J.Cam1.6 and MOLT-4 clone 12) and ZAP70 deficient (P116) T-ALL cells. Histone H3 (H3) expression used as loading control. D)

Dose response curves following single drug and combination therapy in LCK or ZAP70 deficient cells after 72h of treatment assessed by CellTiter-Glo. Error bars +/- SEM. n=3 samples/data point. Not significant (ns) by Student's two-tailed t-test.

Figure 4. Combination dasatinib and temsirolimus inhibits MCL-1 expression. A) Western blot analysis of Jurkat, MOLT-4 and PF-382 T-ALL cells following drug treatment for 120 hours. Representative blot from three biological replicates. GAPDH expression used as loading control. B) Dose response curves following single drug and combination therapy. Dasatinib, temsirolimus and MCL-1 inhibitor AZD5991, after 24 hours of treatment and assessed by CellTiter-Glo. Combination indexes for ED50 concentrations are shown (not significant if ≥ 0.5). C) AZD5991 potently kills T-ALL cells after 4 days of treatment. AZD5991 (250 nM), dasatinib (500 nM), temsirolimus (2μM). Error bars +/- SEM. n=3 samples/data point. *p<0.05, **p<0.01, ***p<0.001, ****p<0.0001 by Student's two-tailed t-test.

Figure 5. Primary human T-ALL cells are killed by dasatinib and temsirolimus combination treatment. A,B) Quantification of combination therapy responses in *ex vivo* treated patient-derived xenograft cells isolated directly from the spleen of leukemic mice. Dose response curves following 72 hours of therapy treatment (A). Quantification of phosphorylated LCK+/S6K+ T-ALL cells for PDX 42512 and PDX TA10 following 30 minutes of drug treatment or 24 hours for PDX 44179 and PDX 24836 (B). Error bars denote +/-STD in A and +/-SEM in B, n=3 replicates per data point and green lines denote synergistic combination treatments. *p<0.05, **p<0.01, ***p<0.001 by two-tailed Student's t-test. Not significant (ns). C-D) Primary patient samples following *ex vivo* combination treatment for 48 hours (ALLT-323, ALLT-373 and ALLT-5221) or 72 hours (ALLT-379, ALLT-6787 and ALLT-7891). Dose response curves with green lines denote synergistic drug responses (C, average across duplicate samples shown). Synergy plots showing

responses of drugs over varied dosing (D). Synergy scores were assigned using the Loewe method and significance of >10 denoting marked synergy (ALLT-323, ALLT-379, ALLT-373, and ALLT-6787).

Figure 6. Combination of dasatinib and temsirolimus inhibit Jurkat T-ALL growth in mouse xenografts. A) Schematic of experimental design. B) Representative images of NSG mice engrafted with luciferase+/dsRED2+Jurkat cells prior to the first day of treatment (day 0) or imaged after treatment on the days noted within each image panel. C) Kaplan-Meier survival curves. Combination treated mice had significant survival benefit when compared to non-treated or mono-therapy treated mice (* $p<0.05$, ** $p < 0.01$, Log-rank, Mantel-Cox test). D) Average radiance of each individual mice measured by bioluminescence. Squares denote the last radiance measurement of moribund animals. Two of six combination-treated mice had undetectable leukemia burden at 60 days. * $p<0.05$, *** $p<0.001$; by Tukey's post-hoc analysis. E) Quantification of dsRed+ T-ALL cells by flow cytometry analysis of the spleen, bone marrow (BM) and peripheral blood from engrafted mice. Error bars equal +/- SEM. *$p<0.05$, ** $p<0.01$ by Tukey's post-hoc analysis. F) Histopathological analysis of spleens from control and combination therapy treated mice. Hematoxylin and Eosin (H&E), TUNEL and co-immunohistochemistry for human CD45 (hCD45, FITC) along with either phospho-LCK or phospho-S6K (Alexa Fluor-594) and DAPI (blue). Scale bars equal 20μm. Arrows show representative stained cells. G) Quantification of IHC analysis of spleens denoting the total number of hCD45 T-ALL cells/3mm^2 across replicates (left) and TUNEL (right). The average percentage of positive cells ± SEM is noted. (H) Quantification of phospho-LCK or phospho-S6K staining in CD45+ T-ALL cells found in the spleen based on IHC staining. Average intensity is denoted by red bars quantified across >3 animals per condition and 3 sections/spleen. > 3,000 cells were analyzed per condition (G,H). **, $p<0.01$, ****, $p< 0.0001$; by Student's two-tailed t-test (G,H).

Figure 7. Combination of dasatinib and temsirolimus suppresses T-ALL growth in patient-derived xenografts. A) Schematic of experimental design. B-F) PDX 441979. G-K) PDX 24836. B,G) Leukemia burden assessed by the percentage of CD45+ T-ALL in the peripheral blood of engrafted mice. Combination therapy curbed tumor growth when compared to control treated mice. p-values denote differences based on one-way ANOVA followed by Tukey post-hoc test. C,H) Kaplan-Meier survival curves. (* $p<0.05$, ** $p<0.01$, *** $p<0.001$, Log-rank, Mantel-Cox test). D,I) Flow cytometry quantification of hCD45+ T-ALL cells detected in the spleen, bone marrow (BM) and peripheral blood of engrafted mice at the end of treatment. Error bars equal +/- SEM. E,J) Quantification of spleen sections showing total number of hCD45 T-ALL cells/3mm^2 (left) and TUNEL (right). Error bars denote ± STD. ,F,K) Quantification of phospho-LCK or phospho-S6K staining in CD45+ T-ALL cells found in the spleen based on IHC staining. Average intensity is denoted by red bars quantified across >3 animals per condition and 3 sections/spleen. > 3,000 cells were analyzed per condition. *$p<0.05$, ** $p<0.01$, *** $p<0.001$, **** $p<0.0001$; Student's two-tailed t-test (D-F,I-K).

Figure 1.

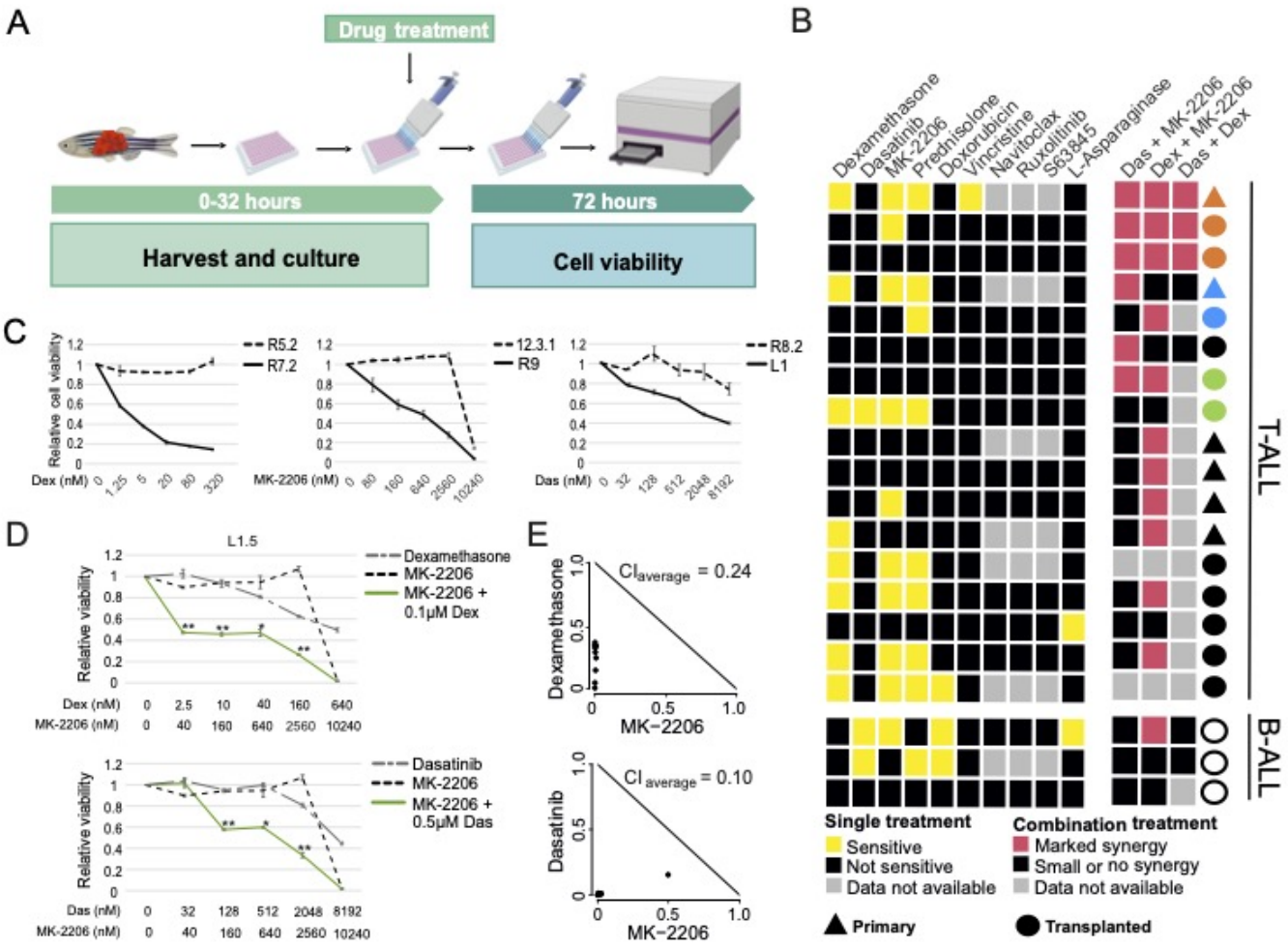
A
Drug treatment
0-32 hours
72 hours
Harvest and culture
Cell viability
B
Dexamethasone
Dasatinib
MK-2206
Prednisolone
Doxorubicin
Vincristine
Navitoclax
Ruxolitinib
S63845
L-Asparaginase
Das + MK-2206
Dex + MK-2206
Das + Dex
T-ALL
B-ALL
Single treatment
Sensitive
Not sensitive
Data not available
Combination treatment
Marked synergy
Small or no synergy
Data not available
Primary
Transplanted
C
Relative cell viability
R5.2
R7.2
12.3.1
R9
R8.2
L1
Dex (nM)
MK-2206 (nM)
Das (nM)
D
L1.5
Relative viability
Dexamethasone
MK-2206
MK-2206 + 0.1μM Dex
Dasatinib
MK-2206
MK-2206 + 0.5μM Das
E
CI average = 0.24
CI average = 0.10
Dexamethasone
Dasatinib
MK−2206

Figure 2.

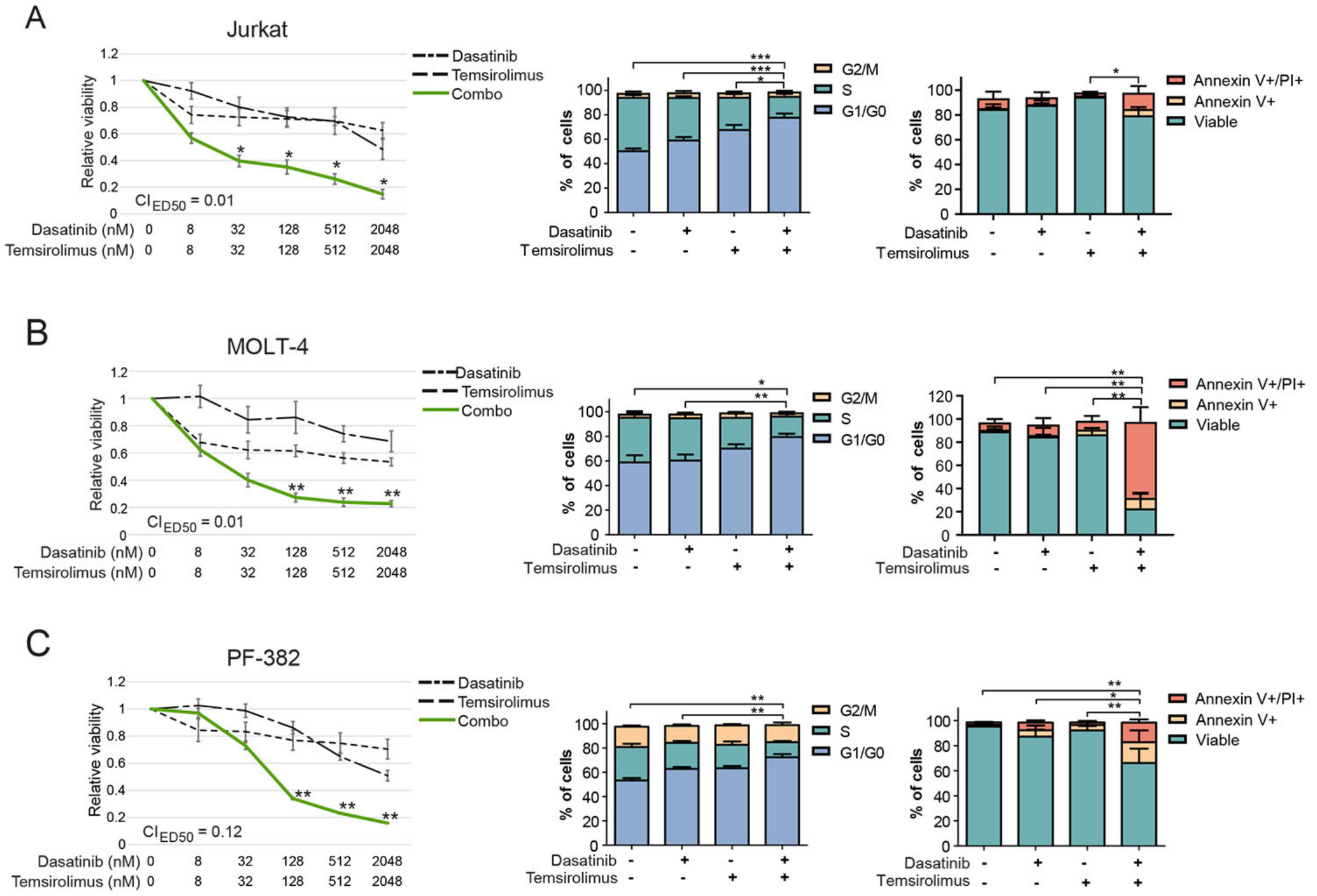
A
Jurkat
Relative viability
Dasatinib
Temsirolimus
Combo
CI ED50 = 0.01
Dasatinib (nM) 0 8 32 128 512 2048
Temsirolimus (nM) 0 8 32 128 512 2048
% of cells
G2/M
S
G1/G0
Dasatinib
Temsirolimus
Annexin V+/PI+
Annexin V+
Viable
B
MOLT-4
CI ED50 = 0.01
C
PF-382
CI ED50 = 0.12

Figure 3.

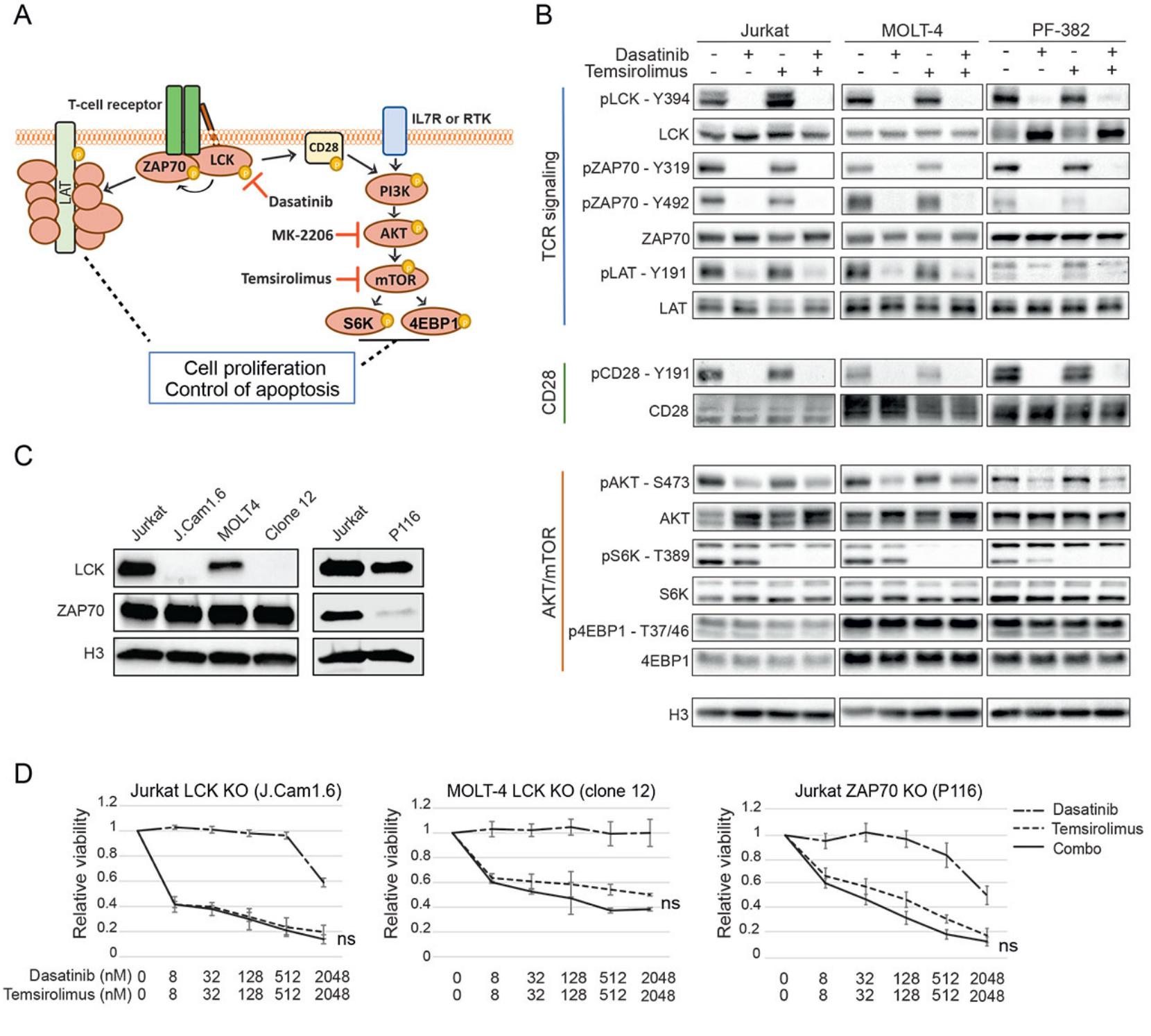
A
T-cell receptor
IL7R or RTK
ZAP70
LCK
CD28
LAT
Dasatinib
PI3K
MK-2206
AKT
Temsirolimus
mTOR
S6K
4EBP1
Cell proliferation
Control of apoptosis
B
Jurkat
MOLT-4
PF-382
Dasatinib
Temsirolimus
TCR signaling
pLCK - Y394
LCK
pZAP70 - Y319
pZAP70 - Y492
ZAP70
pLAT - Y191
LAT
CD28
pCD28 - Y191
CD28
AKT/mTOR
pAKT - S473
AKT
pS6K - T389
S6K
p4EBP1 - T37/46
4EBP1
H3
C
Jurkat
J.Cam1.6
MOLT4
Clone 12
Jurkat
P116
LCK
ZAP70
H3
D
Jurkat LCK KO (J.Cam1.6)
MOLT-4 LCK KO (clone 12)
Jurkat ZAP70 KO (P116)
Relative viability
Dasatinib
Temsirolimus
Combo
ns
Dasatinib (nM) 0 8 32 128 512 2048
Temsirolimus (nM) 0 8 32 128 512 2048

Figure 4.

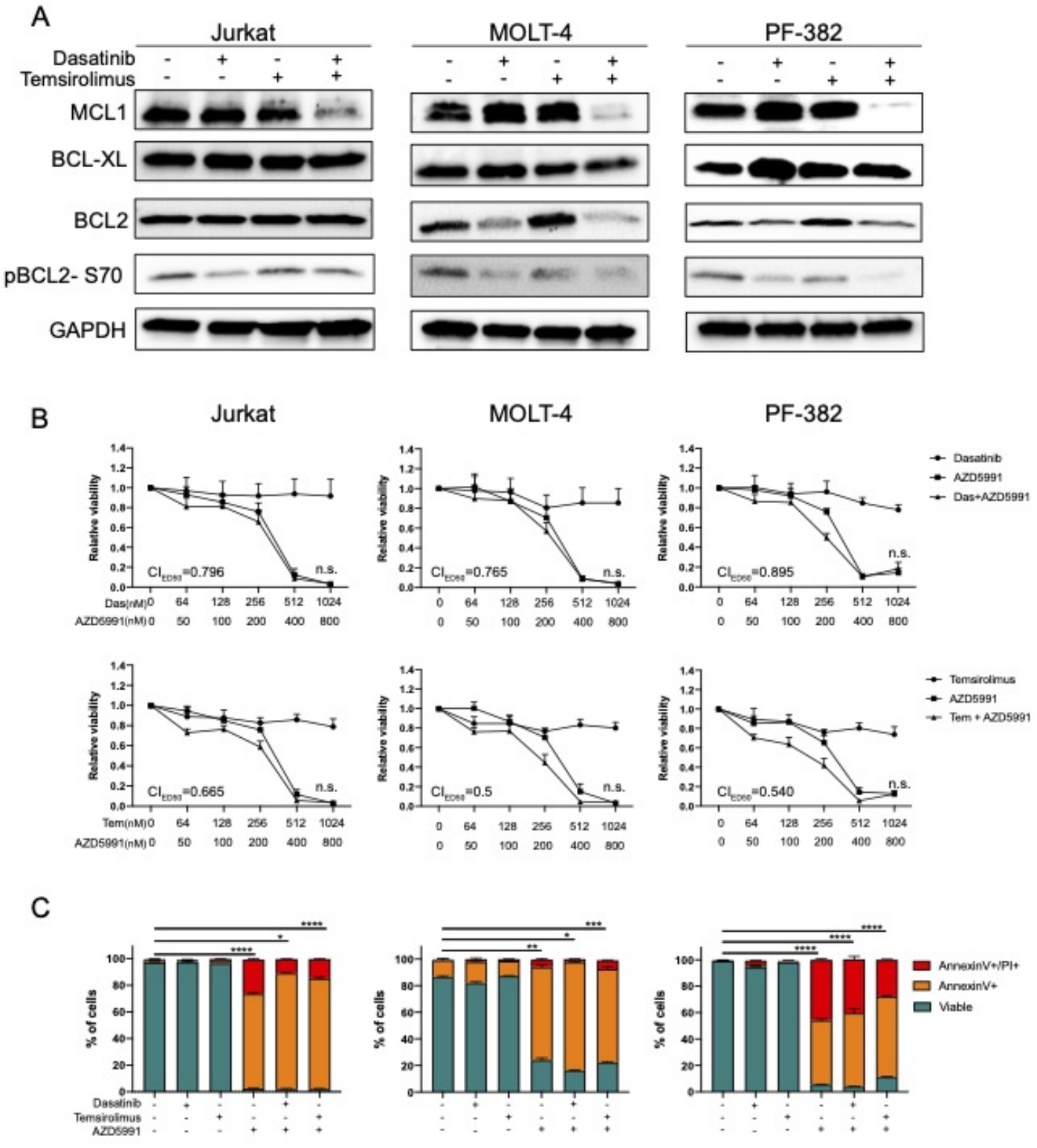
A
Jurkat
MOLT-4
PF-382
Dasatinib
Temsirolimus
MCL1
BCL-XL
BCL2
pBCL2- S70
GAPDH
B
Jurkat
MOLT-4
PF-382
Relative viability
Dasatinib
AZD5991
Das+AZD5991
Temsirolimus
Tem + AZD5991
n.s.
Das(nM) 0 64 128 256 512 1024
AZD5991(nM) 0 50 100 200 400 800
Tem(nM) 0 64 128 256 512 1024
C
% of cells
AnnexinV+/PI+
AnnexinV+
Viable
Dasatinib
Temsirolimus
AZD5991

Figure 5.

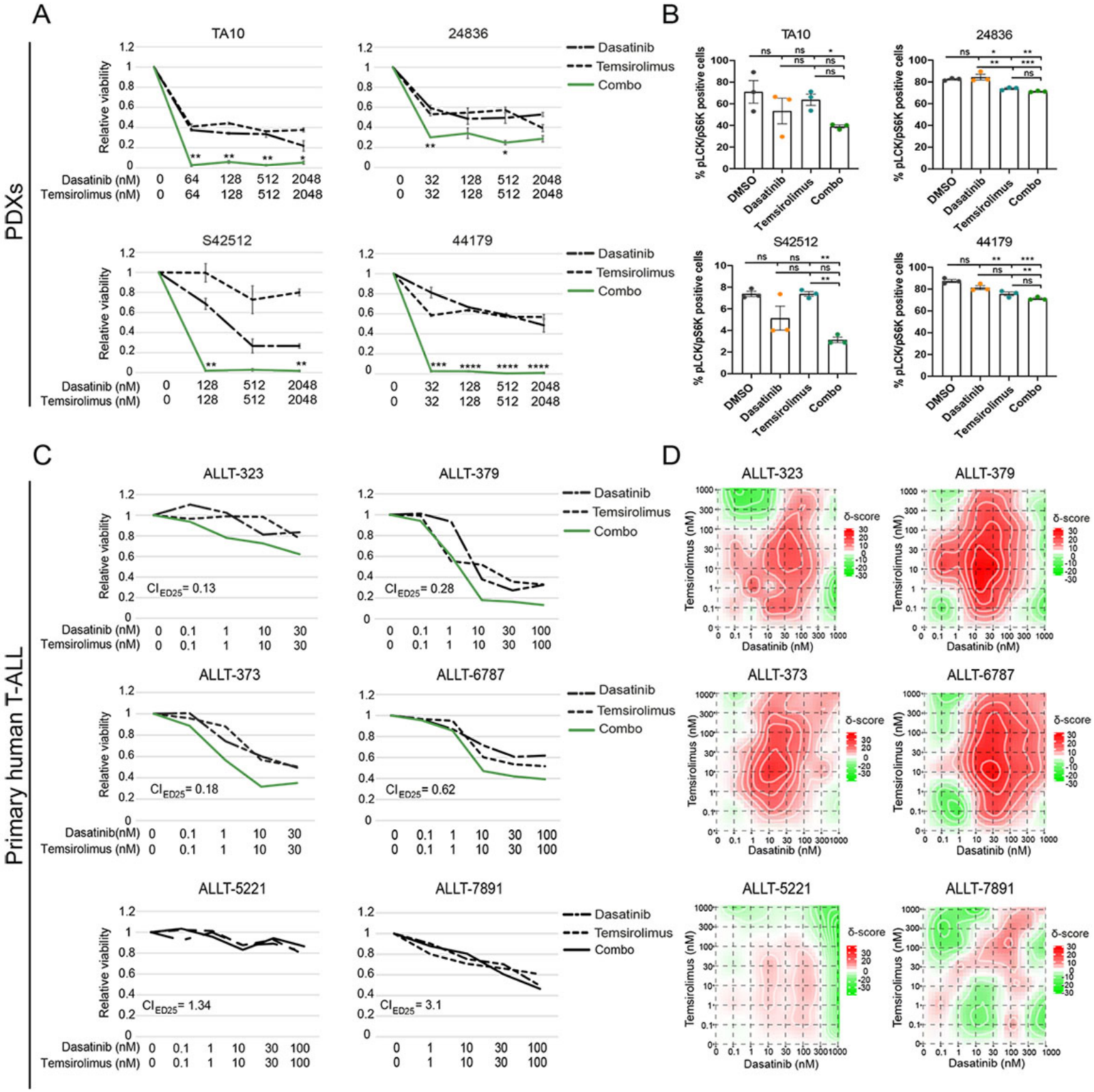
A
PDXs
TA10
24836
S42512
44179
Relative viability
Dasatinib
Temsirolimus
Combo
Dasatinib (nM)
Temsirolimus (nM)
B
% pLCK/pS6K positive cells
DMSO
Dasatinib
Temsirolimus
Combo
C
Primary human T-ALL
ALLT-323
ALLT-379
ALLT-373
ALLT-6787
ALLT-5221
ALLT-7891
CI ED25 = 0.13
CI ED25 = 0.28
CI ED25 = 0.18
CI ED25 = 0.62
CI ED25 = 1.34
CI ED25 = 3.1
D
Temsirolimus (nM)
Dasatinib (nM)
δ-score

Figure 6.

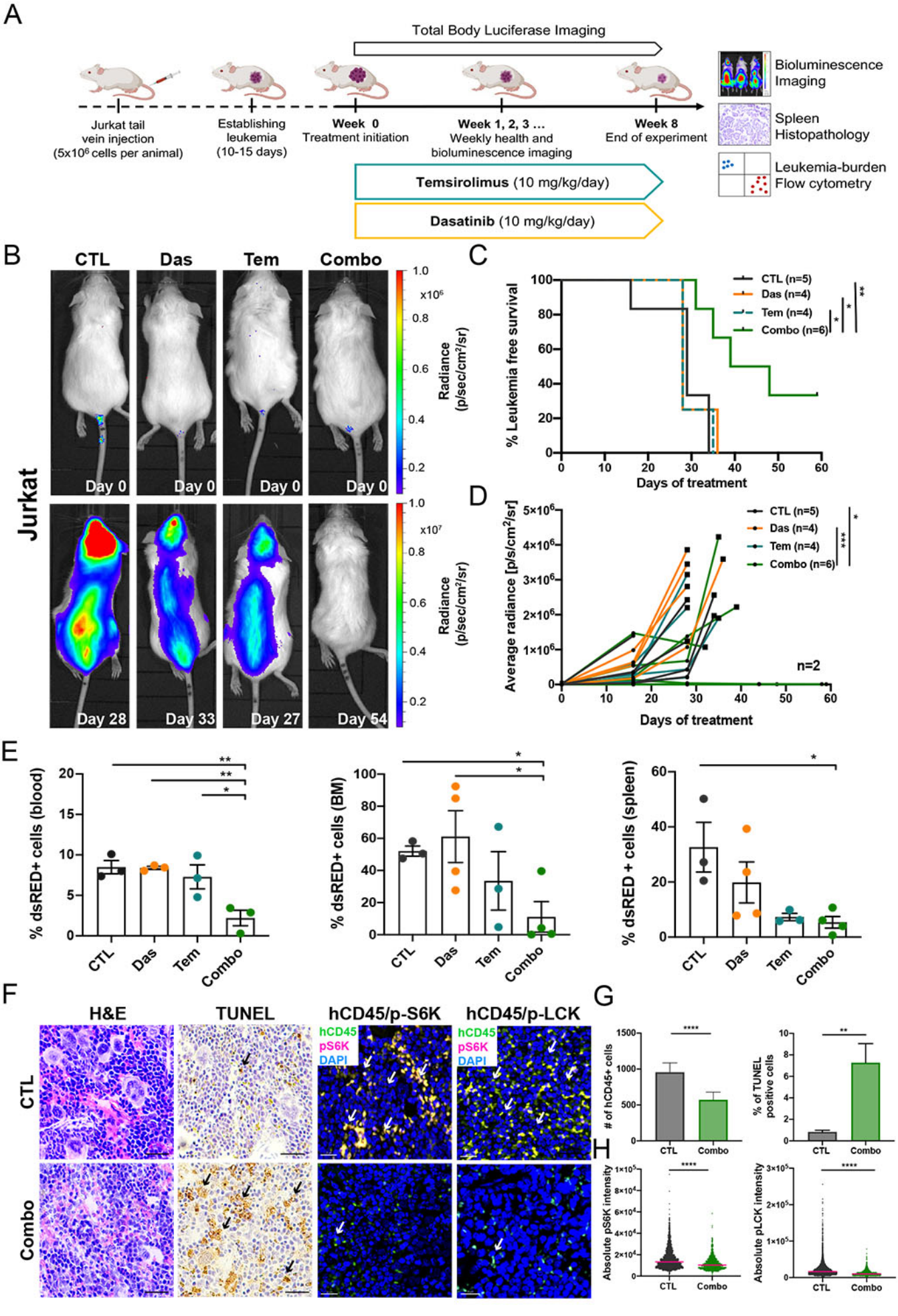
A
Total Body Luciferase Imaging
Jurkat tail vein injection (5x10⁶ cells per animal)
Establishing leukemia (10-15 days)
Week 0 Treatment initiation
Week 1, 2, 3 … Weekly health and bioluminescence imaging
Week 8 End of experiment
Bioluminescence Imaging
Spleen Histopathology
Leukemia-burden Flow cytometry
Temsirolimus (10 mg/kg/day)
Dasatinib (10 mg/kg/day)
B
CTL
Das
Tem
Combo
Jurkat
Day 0
Day 28
Day 33
Day 27
Day 54
Radiance (p/sec/cm²/sr)
C
% Leukemia free survival
Days of treatment
CTL (n=5)
Das (n=4)
Tem (n=4)
Combo (n=6)
D
Average radiance [p/s/cm²/sr]
n=2
E
% dsRED+ cells (blood)
% dsRED+ cells (BM)
% dsRED + cells (spleen)
F
H&E
TUNEL
hCD45/p-S6K
hCD45/p-LCK
hCD45
pS6K
DAPI
G
# of hCD45+ cells
% of TUNEL positive cells
H
Absolute pS6K intensity
Absolute pLCK intensity

Figure 7.

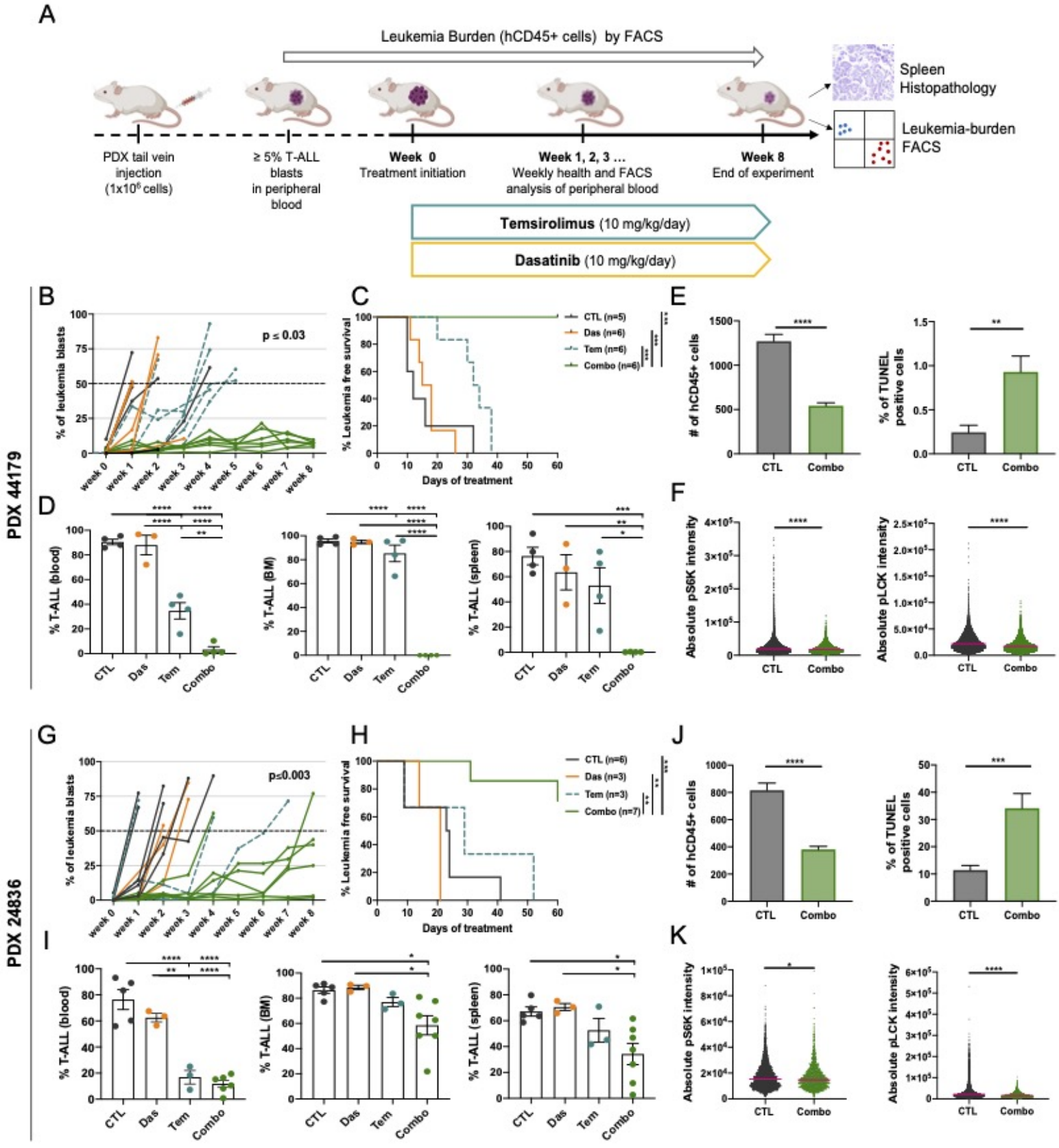
A
Leukemia Burden (hCD45+ cells) by FACS
Spleen Histopathology
Leukemia-burden FACS
PDX tail vein injection (1x10^6 cells)
≥ 5% T-ALL blasts in peripheral blood
Week 0 Treatment initiation
Week 1, 2, 3 … Weekly health and FACS analysis of peripheral blood
Week 8 End of experiment
Temsirolimus (10 mg/kg/day)
Dasatinib (10 mg/kg/day)
PDX 44179
B
% of leukemia blasts
p ≤ 0.03
C
% Leukemia free survival
Days of treatment
CTL (n=5)
Das (n=6)
Tem (n=6)
Combo (n=6)
E
# of hCD45+ cells
% of TUNEL positive cells
CTL
Combo
D
% T-ALL (blood)
% T-ALL (BM)
% T-ALL (spleen)
F
Absolute pS6K intensity
Absolute pLCK intensity
PDX 24836
G
p≤0.003
H
CTL (n=6)
Das (n=3)
Tem (n=3)
Combo (n=7)
J
K
I